RSC Advances

PAPER

View Article Online
View Journal | View Issue

Cite this: *RSC Adv.*, 2020, **10**, 8810

Spectroscopic demonstration of sinapic acid methyl ester complexes with serum albumins†

Adam Kasparek * and Bogdan Smyk

Received 28th November 2019
Accepted 6th February 2020

DOI: 10.1039/c9ra09980h

rsc.li/rsc-advances

The methyl ester of sinapic acid (MESA) is a molecule with confirmed antioxidant properties. It is important to establish whether it can be transported across humans and animals. Therefore, we investigated MESA interactions with serum albumins, namely, human serum albumin (HSA), bovine serum albumin (BSA), rabbit serum albumin (RSA), and sheep serum albumin (SSA). Experiments were performed in a pH range from 5.9 to 10.7 using absorption and fluorescence techniques. It was found that MESA formed complexes with every albumin in the entire pH range under examination, which was confirmed by the appearances of new absorption and fluorescence complex bands. Fluorescence intensities were much higher (up to 20 times) and lifetimes were up to 340 times as compared to those for unbound MESA. The quenching experiments at pH 7.4 showed that the stoichiometry for every albumin was 1 : 1; the binding constant was the highest for HSA, which reached 52 000 M^{-1}. The obtained results suggested that MESA preferred the hydrophobic binding sites in albumins. The analysis of the fluorescence spectra and fluorescence lifetimes showed two possibly different binding sites in BSA, RSA, and SSA as well as three binding sites in HSA.

Introduction

Recently, natural antioxidants have been used to extend the shelf lives of human food and animal feed. Natural candidates comprise compounds having one or more phenolic groups in their molecular structures. These include, among others, sinapic acid (Sa), which is a representative of hydroxycinnamic acids. Hydroxycinnamic acids have many important biological functions including antioxidative, antimicrobial, and cancer-preventing functions.[1] Sa is one of the best antioxidants among them.[2–5] It occurs in many plants, such as vegetables and cereals (mainly in rapeseed),[6–8] which causes it to be consumed by humans as well as animals. In the body, it is absorbed in the small intestine,[9] from which it enters the blood plasma and then, it can be transported by forming molecular complexes with albumins.[10] In plants, Sa exists in the free form and in the form of esters, including methyl ester (methyl ester of Sa (MESA); Chart 1).

MESA is, for example, the main component of a radish methanolic extract.[7,11] According to some reports,[3,12] MESA has greater antioxidant potential than Sa. The same was confirmed by Gaspar and others,[13] who compared the antioxidant abilities of various phenolic acids to their esters. MESA acts as an antioxidant *via* the dehydrogenation of a hydroxyl group at the ring or by electron transfer.[13] Because MESA is a strong antioxidant, there is a chance that in the future, it will be added to food and feed to prevent their spoilage. For this reason, it is likely that it will circulate in the body.[14,15] However, until now, there have been no reports on whether MESA can be transported by proteins in the organism. The natural candidates for MESA transport are serum albumins. One of their functions in the body is aiding the transport and distribution of various molecules, including hormones and fatty acids.[16–20] In our previous work,[21] we determined the physical and chemical properties of MESA in different microenvironments: the pK_a values in the ground and excited states (8.6 and 1.9, respectively), fluorescence lifetimes in water as well as polar and nonpolar solvents, and quantum yields (QYs). It was also found that MESA could be dissolved in a wide pH range (from 2 to 11). The main goal of this study was to investigate whether MESA forms molecular complexes with serum albumins or not and whether it can be transported with them or not. This is because in preliminary studies, the fluorescence quantum efficiency was greater in the presence of BSA than that without it, which suggested complex

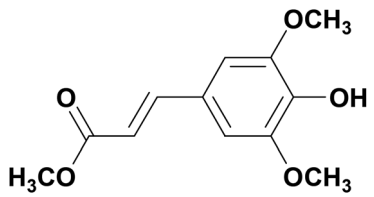

Chart 1 Molecular structure of MESA.

Department of Physics and Biophysics, University of Warmia and Mazury in Olsztyn, Oczapowskiego 4, 10-719 Olsztyn, Poland. E-mail: adam.kasparek@uwm.edu.pl

† Electronic supplementary information (ESI) available. See DOI: 10.1039/c9ra09980h

formation. We determined the pH values at which it is the most effective in the case of four albumins, namely, bovine serum albumin (BSA), human serum albumin (HSA), rabbit serum albumin (RSA), and sheep serum albumin (SSA). Another issue is whether MESA can be used as a fluorescent probe for serum albumins or not, particularly at alkaline pH (above 10).

Materials and methods

Materials

Sa, BSA, HSA, RSA, and SSA were purchased from Sigma-Aldrich (Poland). MESA was prepared in the same way as that in an earlier work[21] according to the procedure described by Fujita *et al.*[22] Stock solutions of MESA (0.3 mM) and albumins (0.2 mM) were prepared in water from the Millipore Simplicity 185 ultrapure water purification system. The final solutions were obtained by adding 0.5 mL of MESA solution, 0.5 mL of the appropriate albumin solution, and 9 mL of PBS or carbonate buffer at the appropriate pH, resulting in a final concentration of 15 μM of MESA and 10 μM of the corresponding albumin. For quenching experiments, a stock solution of MESA (0.5 mM) and albumin (50 μM) was prepared in a PBS buffer at pH 7.4. Then, albumin was diluted to the final concentration of 5 μM with a buffer and MESA solution. The final MESA concentration was in the range of 2.5–50 μM.

Methods

The absorption spectra were measured by means of a Cary 5000 spectrophotometer and the fluorescence spectra by using a Cary Eclipse spectrofluorometer (Agilent, Australia). The emission and excitation slits were set to 10 nm. The measurements were carried out in a 1 cm quartz cuvette using right-angle geometry. A temperature of 298 K was set for both the instruments using the Peltier accessory. The emission spectra were determined at excitation wavelengths, λ_{ex}, of 375, 390, and 410 nm, and λ_{ex} = 280 nm was used for the quenching experiment, whereas the excitation spectra were determined at the observation wavelength, λ_{em}, of 480 nm. The fluorescence spectra were corrected for the sensitivity of the instrument as well as for the inner filter effects of type I and II according to the procedure described by Kasparek and Smyk.[23] The fluorescence lifetimes were measured with a FluoTime 200 spectrophotometer (PicoQuant, Germany) with a TCSPC module and an MCP PMT detector with an electron transit time of 25 ps as well as a FluoTime 300 spectrophotometer (PicoQuant, Germany) with a hybrid PMT detector for an electron transit time of 50 ps. The samples were excited with a 375 nm laser diode (PicoQuant, Germany) and with a 280 nm LED diode (PicoQuant, Germany). The pH value was measured using a Jenway 3030 (United Kingdom) pH meter. The calculations were carried out using the following software: MATLAB v. 2014 (MathWorks, USA), GraphPad Prism 7.05 (GraphPad Software, USA), PeakFit 4.04 (Systat Software Inc., USA), and FluoFit 4.6.6 and EasyTau 2.1 (PicoQuant, Germany).

Gaussian decomposition of the fluorescent spectra

The Gaussian decompositions of the fluorescence spectra were performed using the PeakFit software. The MESA spectrum without albumin was subtracted from the fluorescence spectra, and the Savitzky–Golay method was used for smoothing. The "Log Normal Area" peak type for the excitation spectra and the "Gauss Area" for the emission spectra were used. The criterion determining the number of peaks was the minimization of standard deviation (SD) and R^2.

Reconvolution of exponential decays

Fluorescence decays were analyzed using the FluoFit and EasyTau software. The fluorescence decays were fitted using the sum of the exponential terms:

$$I(t) = \int_{-\infty}^{t} \mathrm{IRF}(t') \sum_{i=1}^{n} \alpha_i e^{-\frac{t-t'}{\tau_i}} dt' \quad (1)$$

where IRF(t') is a function of the response devices at time t'. Further, α_i is the amplitude of the decay of the i^{th} component, and τ_i is the lifetime. The criterion of match quality was χ^2 checked using the built-in tools in the FluoFit software.

Stern–Volmer and FRET analyses

The results obtained from the quenching experiment were fitted to the Stern–Volmer equation:[24]

$$\frac{F_0}{F} = 1 + K_{SV}[Q] = 1 + k_q \tau_0 [Q] \quad (2)$$

where F_0 is the fluorescence of albumin without MESA, F is the fluorescence of albumin at Q concentration of MESA at λ_{em} = 350 nm, K_{SV} is the Stern–Volmer quenching constant, k_q is the bimolecular quenching constant, and τ_0 is the fluorescence lifetime of albumin without MESA.

In order to determine the binding constant, K_b, we fitted the obtained results to the following equation:[25–27]

$$\log\left[\frac{F_0 - F}{F}\right] = \log[K_b] + n \log[Q] \quad (3)$$

where n is the number of binding sites.

In order to calculate the distances between MESA and tryptophan (Trp) in the albumins, the following equation for determining the Förster distance, R_0, was used:[24]

$$R_0 = 0.211(\kappa^2 n^{-4} \mathrm{QY_A} J(\lambda))^{1/6} \quad (4)$$

where κ is the factor describing the relative orientation in space between the albumins and MESA and is assumed to be equal of 2/3,[24] n is the refractive index of the solution and is equal to 1.36, QY_A is the QY of the serum albumin and is calculated by using the methods described by Kasparek and Smyk,[23] $J(\lambda) = \frac{\int_0^\infty F_0(\lambda)\varepsilon_M(\lambda)\lambda^4 d\lambda}{\int_0^\infty F_0(\lambda) d\lambda}$, and ε_M is the absorption coefficient of MESA. Distance, r, between the Trp and MESA was calculated using the following equation:[24]

$$E = 1 - \frac{F}{F_0} = \frac{{R_0}^6}{{R_0}^6 + r^6} \quad (5)$$

where E is the efficiency of energy transfer.

Results and discussion

Absorption of MESA solutions with proteins

Based on the results of the preliminary research and albumin properties, it was expected that MESA would form complexes with them. In addition, several types of complexes were expected due to the number of potential binding sites for albumin.[19,20,28] The absorption of MESA solutions with albumin was measured in the pH range from 5.9 to about 10.9. Fig. 1 shows the exemplary absorption spectra of MESA and SSA solutions. In this figure, the solid lines represent the MESA spectra with the protein and dashed lines without protein. The spectra of the solutions with the highest pH value are marked in blue color and those with the lowest pH value are denoted in red color. Based on the above results, the MESA spectra in the presence of SSA at the extreme pH values were calculated using software[29] and are shown in Fig. S1.† The description of the spectra are the same. Both these figures show changes in the MESA absorption spectra after SSA addition, which can be attributed to the absorbance reduction at the maximum of the undissociated form at 322 nm and the appearance of a small band at around 410 nm. In the case of the dissociated form, a bathochromic shift of about 3 nm was observed. These results indicate that in the electronic ground state, MESA forms complexes with the SSA. Similar spectra were obtained for the remaining albumins (Fig. S2†). The pK_a value of the OH group in the MESA ground state without proteins was 8.6 ± 0.2.[21] The calculated pK_a values of the MESA solutions with albumins are listed in Table 1. The observed changes relative to the MESA without proteins were relatively small and were within the limits of the measurement error. However, the pK_a value decreased for each albumin, suggesting a weak effect of binding sites on the dissociation of the hydroxyl group of the MESA—there was no significant weakening in protein binding. Therefore, the fraction of the residues of the polypeptide side chain of the polar amino acids involved in the binding was negligible. In addition, while the MESA alone was unstable at higher pH, the addition of albumins significantly increased its stability.

Table 1 pK_a values of MESA solutions with different albumins[a]

MESA with	pK_a ± SD
HSA	8.24 ± 0.47
BSA	8.50 ± 0.61
RSA	8.48 ± 0.49
SSA	8.40 ± 0.70

[a] SD: standard deviation.

Fluorescence of MESA with HSA

Excitation and emission spectra. MESA solutions with and without HSA at increasing pH values were excited at 375, 390, and 410 nm. Fig. 2 shows the emission spectra of these solutions at λ_{ex} = 375 nm. The red solid line indicates the spectrum of MESA with protein plotted for the lowest pH (5.9), the blue solid line for the highest pH (10.9), and the green line for the spectrum with the highest intensity. The dashed lines in colors as mentioned above denote the MESA spectra without protein. The intensity of the MESA band without protein at pH 5.9 was so small that it was practically invisible in this figure. The increase in the fluorescence intensity of MESA with HSA solutions occurred up to pH 9.56 and was followed by a decrease. At pH 9.56, this increase was about 20-fold in relation to the band intensity of MESA without HSA. The wavelength of 375 nm mainly excited the complexes in the dissociated form, the concentration of which increased with the pH. Therefore, the observed increases in intensity were associated with this form of MESA. The decrease in fluorescence intensity at high pH could be probably associated with an increase in the negative charge of both HSA[30] and MESA. Above pH 11, electrostatic repulsion and albumin unfolding may prevent the formation of complexes. The maximum portion of the emission spectra exhibits a hypochromic shift with increasing pH, but this shift was smaller in the presence of a protein. The maximum obtained with the protein varied from 459 nm at pH 5.9 to 472 nm

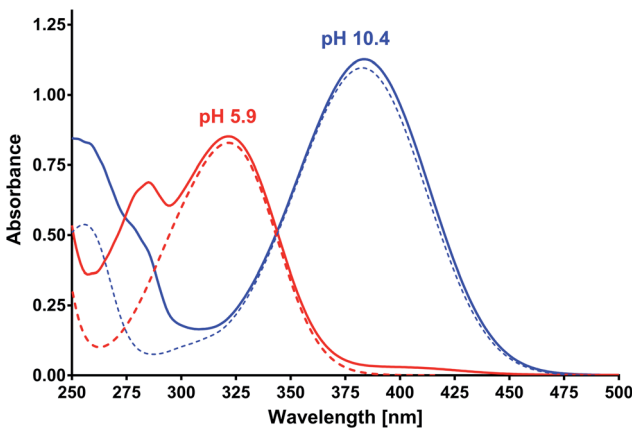

Fig. 1 Absorption spectra of MESA with (dashed line) and without HSA (solid line) *versus* pH. Concentration of MESA: 15 μM; concentration of SSA: 10 μM; path length: 1 cm. Red line: pH 5.9; blue line: pH 10.4.

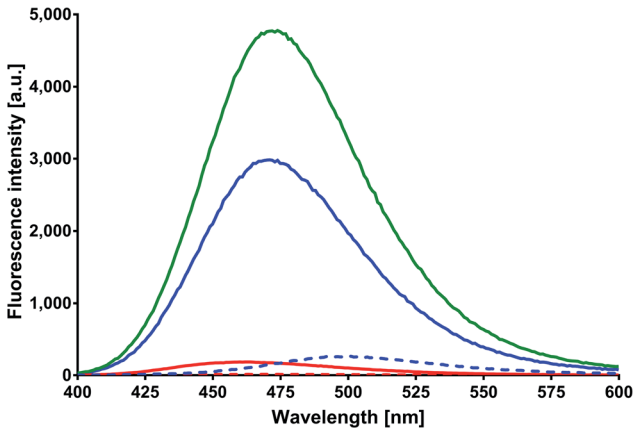

Fig. 2 Corrected fluorescence spectra of MESA with (dashed line) and without HSA (solid line). Concentration of MESA: 15 μM; concentration of HSA: 10 μM; λ_{ex} = 375 nm; 1 cm quartz cell; right-angle geometry. Red line: pH 5.9; blue line: pH 10.9.

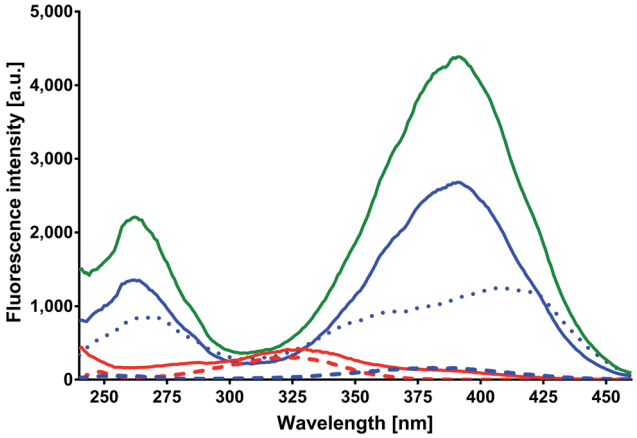

Fig. 3 Corrected fluorescence excitation spectra of MESA with (dashed line) and without HSA (solid line). Concentration of MESA: 15 μM; concentration of HSA: 10 μM; λ_{ex} = 375 nm; 1 cm quartz cell; right-angle geometry. Red line: pH 5.9; blue line: pH 10.9.

at pH greater than 9.5. Similar shifts were observed for MESA without proteins when changing the polarity of the organic solvents from polar to nonpolar.[21] This implies the participation of hydrophobic binding sites of HSA in complexes formation. Qualitatively, the same results were obtained for the other excitation wavelengths. Fig. 3 shows the excitation spectra of MESA solutions with and without the protein corrected and not corrected for the inner filter effect. The blue dotted line represents an example of the raw spectrum at pH 10.9 in order to demonstrate the importance of spectral corrections. Spectrum markings are the same as those shown in Fig. 2. Similar to the emission spectra, the fluorescence intensity increases with pH increasing to 9.6 and then decreases. The excitation maximum for the dissociated form is 391 nm; therefore, there was a marginal shift of about 8 nm toward longer wavelengths. This result is consistent with the results obtained from the absorption spectra, thereby confirming the existence of MESA with HSA complexes in the electronic ground state.

QT and lifetime. For all the pH values, QYs were determined using the method described by Kasparek and Smyk.[23] MESA[21] was used as the reference solution with a known QY. The QYs for the MESA solutions with all the investigated albumins (solid lines) are shown in Fig. 4. The red line and black dashed line show the QYs of MESA with and without HSA, respectively. The highest QY was achieved at pH 6.8, which was 0.0176 ± 0.0015. In the entire pH range under consideration, QY was slightly decreasing. The average value varied around 0.015 with the accuracy of measurement error. Only for pH > 10.5, there was a significant decrease in the value, which was 0.0083 ± 0.0001. When comparing these results with the data regarding albumins,[21] the increase was about 8–10-fold for pH below pK_a and near 20-fold for pH above pK_a. This significant increase, occurring also at alkaline pH, suggests that MESA can be used as a fluorescent probe over the entire pH range above 6, particularly at alkaline pH.

For all the pH values of the solutions, the fluorescence decay times were measured and reconvoluted using the "Global Method" for the four observation wavelengths. They are listed in Table 2. The best matches were obtained when using the triple-exponential decay. All the lifetimes of MESA with HSA were many times greater than those of MESA without HSA. This suggests the presence of three different binding sites in HSA, because the protein has no absorption bands for the excitation wavelength of 375 nm and the lifetimes of both the MESA forms were very low, *i.e.*, below 10 ps.

Spectral decomposition. In order to obtain the quantitative data regarding the complexes of MESA with HSA, the fluorescence spectra were decomposed over Gaussian curves. In the subsequent text, the term "binding sites" will be used interchangeably with the term "complex." The decomposition results are shown in Fig. 5, S3 and S4.† Fig. 5 shows the maxima wavelengths, and Fig. S3† shows the intensities of the Gaussian peaks as a function of pH. The light green and light blue colors highlight the maxima of the MESA without protein of the dissociated (λ_{max} = 500 nm) as well as undissociated (λ_{max} = 464 nm) forms, respectively. In Fig. 5, S3 and S4,† binding site 1 (KH1) with maxima in the range of 480–500 nm is marked in red, binding site 2 (KH2) with the maxima in the range of 450–470 nm is marked in blue, and binding site 3 (KH3) with the maxima below 450 nm is marked in black. The solid lines denote λ_{ex} = 390 nm, dashed lines denote λ_{ex} = 410 nm, and dotted lines indicate λ_{ex} = 375 nm. The Gaussian distributions show that there were 3 complexes; however, KH3 could be

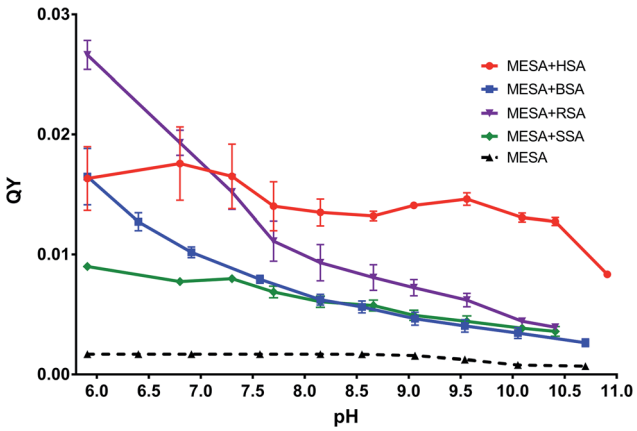

Fig. 4 QY of MESA with and without albumins *versus* pH.

Table 2 Fluorescence decay times of MESA with HSA

pH	τ_1 [ns]	τ_2 [ns]	τ_3 [ns]
5.9	2.557	0.432	0.132
6.8	1.562	0.365	0.115
7.3	1.362	0.353	0.111
7.7	1.356	0.361	0.113
8.2	1.442	0.365	0.105
8.7	1.600	0.382	0.101
9.0	1.754	0.410	0.101
9.6	1.892	0.449	0.107
10.1	1.919	0.453	0.106
10.4	1.927	0.455	0.105

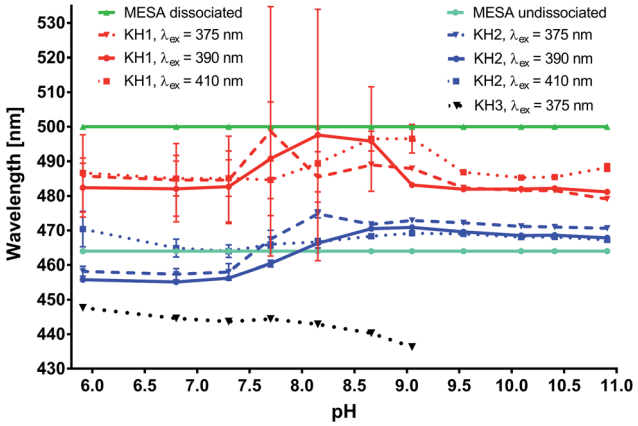

Fig. 5 Changes in the maxima of the complexes from the decomposed fluorescence spectra of MESA with HSA *versus* pH.

excited only for a wavelength lower than 375 nm. This complex was formed only at pH ≤ pK_a. Therefore, it is likely that KH3 was formed by undissociated MESA. The maximum of KH1, with accuracy to its calculation error, was constant over the entire pH range under consideration, which was equal to 482 nm. Fig. S3† shows that the intensity of this complex increased with the pH up to ≈9.5. In the pH range of 9.5–10.5, this value marginally decreased for $\lambda_{ex} = 390$ and 410 nm or remained stable for $\lambda_{ex} =$ 375 nm; however, above pH 10.5, it strongly decreased. In the case of KH2, for every excitation wavelength at pH below pK_a, it was approximately 457 nm; in the vicinity of pK_a, it increased and then reset at 471 nm. The intensity of the KH2 band changed similar to that of KH1, but it reached the maximum at pH 9. The increase in the fluorescence intensities of the KH1 and KH2 complexes with an increase in pH to 9–9.5 was mostly attributed to the decrease in the concentration of undissociated MESA and increase in the concentration of dissociated MESA. A significant decrease above pH 10.5 was most likely because of the strong electrostatic repulsion between the anionic form of MESA and HSA–HSA has a high negative net charge.[30] Despite this, MESA was bound in the hydrophobic site of HSA, which is suggested by the results obtained with MESA in nonpolar solvents.[21] In addition, no complexes of Sa with BSA were formed at this pH[28] because of the double-dissociated form of Sa. Fig. S5 and S6† shows the distribution of the fluorescence excitation spectra to the lognormal peaks. The peak asymmetry was very small, and the peaks were very close to the Gaussian peaks. Similar to the emission spectra, 3 bands were isolated for lower pH (up to 7.7) and 2 bands of complexes for higher pH. The maximum bandwidth of the KH1 complex (red) was in the range from 385 to 395 nm, slightly increasing from pK_a. In the case of KH2 (blue), the maximum shifted toward the longer waves from 328 nm at pH 5.9 to 359 nm at pK_a and then slightly shifted to 368 nm at pH 10.91. The KH3 band with the maximum of about 275 nm (marked in black) could be separated from the protein peak only up to pH 7.7. In order to assign the calculated lifetimes to the individual MESA with HSA complexes, the fluorescence spectra of the complexes were calculated using the f_i coefficients: $f_i = (\alpha_i\tau_i)/\left(\sum_j \alpha_j\tau_j\right)$ corresponds to specific lifetimes. The obtained results indicate that the shapes of the fluorescence spectra corresponding to times τ_2 and τ_3 are the same (Fig. S9†), suggesting that both the lifetimes were associated with the same binding site or two similar binding sites. Fig. S8† shows the fluorescence intensity calculated at the observation wavelength of 480 nm. The solid lines correspond to the intensity of the individual peak obtained from the Gaussian decomposition. The KH1 complex is marked with red line; KH2, blue line; and KH3, black line. The dashed lines indicate the spectral intensities obtained from the multiplication of the fluorescence intensity by factor f_i. The blue line represents the added spectra associated with τ_2 and τ_3. The red line shows the spectrum corresponding to τ_1. The shapes of the blue lines are similar to each other. Red lines are also similar. The same analysis was carried out for the remaining three wavelengths for observations in the measurement of lifetimes. In addition, the shape of the fluorescence peaks obtained by means of lifetimes was compared with that of the spectra obtained from the Gaussian decomposition (Fig. S7†). From the analyses shown in Fig. S7–S9,† it may be concluded that τ_2 and τ_3 represent the same KH2 complex, while τ_1 is linked with the KH1 complex. Since both KH1 and KH2 have a blue-shift in relation to the dissociated form of MESA, we can conclude that both the binding sites are hydrophobic pockets. In the case of KB1, the maximum of both fluorescence and excitation spectra did not change with the increase in pH in the range of the measurement error. Simultaneously, there was a significant 120–250-fold increase in τ_1 as compared to that of the unbound MESA. Because the KH2 maxima changed more with increasing pH than that for KH1 and because the lifetimes increased less (around 40 times), the binding site of KH1 seems to be more hydrophobic than that of KH2. The binding site of KH1 is probably (Sudlow site I) chosen by anions,[20] whereas hydrophobic–hydrophilic site II, occupied by KH2, may be accessed by the solvent molecules. The optional KH2 binding site may be located on the HSA surface. The possibility of binding inside the protein structure is confirmed by the lifetimes, which do not significantly change with increasing pH values.

Fluorescence of MESA with BSA

The solutions of MESA with BSA were excited with the same wavelengths as that in the case of HSA. Fig. 6 shows the emission spectra of MESA with and without BSA for $\lambda_{ex} = 375$ nm. Similar to that in the case of HSA, the solid lines denote the MESA spectra with BSA, where the solid blue line indicates the spectrum for the highest pH (10.70) and the solid red line denotes the spectrum for the lowest pH (5.91). The MESA spectra without protein were marked with dashed lines, where red color was used for the lowest and blue color for the highest pH values. The fluorescence intensities of MESA with BSA increased up to pH 9.5 (green color). However, the increase in fluorescence intensity at pH 9.5 with protein relative to that without protein was lower than that for HSA and was about 4.7. Similarly, with HSA, the increase in fluorescence intensity with

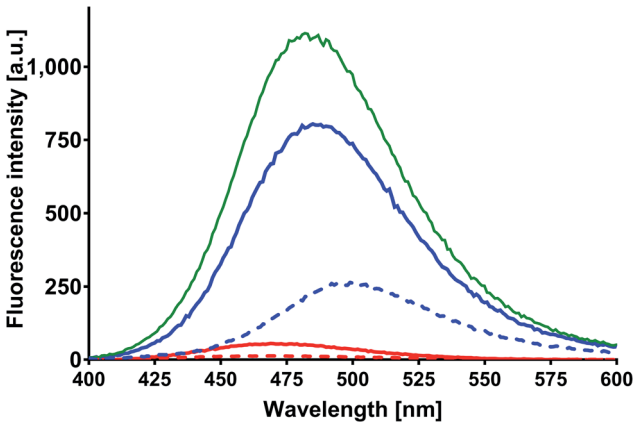

Fig. 6 Corrected fluorescence spectra of MESA with (dashed line) and without BSA (solid line). Concentration of MESA: 15 μM; concentration of BSA: 10 μM; λ_{ex} = 375 nm; 1 cm quartz cell; right-angle geometry. Red line: pH 5.9; blue line: pH 10.9.

increasing pH is associated with an increase in the concentration of the dissociated form, which is the main form excited by the wavelength of 375 nm. The maximum fluorescence intensity for pH 5.9 was 469 nm, which increased with the pH (up to 9.5); above this value, the maximum remained constant at 487 nm. A similar case is seen for HSA: the maximum below 500 nm suggests the binding of MESA to the hydrophobic sites of BSA. The same results were obtained for the other excitation wavelengths. In Fig. 4, the dependence of QYs of the MESA solution with BSA on pH is indicated with blue color. The QYs markedly decreased as the pH increased. The highest QY was determined for the lowest pH (5.9), which was equal to 0.0164 ± 0.0024. The lowest QY value of 0.00262 ± 0.00015 was determined for the solution with the highest pH (10.7). When comparing QYs of MESA with and without the protein in the entire pH range under consideration, the QY of MESA with BSA was found to be significantly higher. Below pK_a, this increase is about 10-fold, whereas above pK_a, it is constant and then decreases to about 3.5. This suggested that MESA can be used as a BSA fluorescent probe. MESA, in contrast to Sa,[28] can form complexes with BSA at alkaline pH (at least up to 10.7), and the QY of fluorescence is about twice as high. In order to extract the complex bands, the MESA fluorescence spectra with BSA were decomposed. The peak maxima obtained are shown in Fig. S10.† The KB1 complex, whose maximum is in the range between 482 and 497 nm, is denoted with the red line, while KB2 having the maximum in the range between 466 and 474 nm was denoted with blue line. The solid line indicates the results for λ_{ex} = 390 nm, dashed line for λ_{ex} = 410 nm, and dotted line for λ_{ex} = 375 nm. The fluorescence maximum of the dissociated form of MESA without protein (λ_{max} = 500 nm) is marked with the light green color. The best fit in the entire pH range was obtained for two bands of complexes and not for three as that in the case of HSA. The existence of the third complex band at pH of about 7.0 cannot be ruled out, because the maximum of KB2 for λ_{ex} = 375 nm (Fig. S10†)—the blue dotted line—exhibited a significant blue-shift. The maximum of KB1 had a smaller blue-shift (from 484 to 497 nm) with increasing pH. The KB2 maximum, initially shifted to 475 nm at pH 6.9, and then practically did not change. The fluorescence decay times were calculated using the global method for the three wavelengths under consideration. The results for all the pH values are shown in Table 3. The best matches were obtained for the triple-exponential decay. All the lifetimes were many times greater than the lifetimes of MESA without BSA. Based on these calculations, τ_1 should be associated with the KB1 complex, whereas τ_2 and τ_3 with the KB2 complex. In contrast to HSA, it cannot be unambiguously determined which of the binding sites are more hydrophobic, as both the maxima and lifetimes were changed with changing pH. However, for KB2, changes in the maximum as well as the lifetime occurred mainly for pH below 7.

Table 3 Fluorescence decay times of MESA with BSA

pH	τ_1 [ns]	τ_2 [ns]	τ_3 [ns]
5.9	3.408	0.636	0.127
6.4	2.595	0.51	0.115
6.9	1.806	0.398	0.101
7.6	1.273	0.319	0.0883
8.2	1.271	0.335	0.0927
8.6	1.268	0.333	0.0903
9.1	1.33	0.378	0.1033
9.5	1.337	0.397	0.108
10.1	1.303	0.400	0.109
10.7	1.298	0.441	0.125

Therefore, if the third complex existed, then the KB2 binding site should be in the interior of the protein and therefore should be highly hydrophobic.

Fluorescence of MESA with SSA

MESA solutions with SSA were excited with the same wavelengths as that used in the previous cases. Fig. 7 shows the emission spectra for λ_{ex} = 375 nm. The solid lines show the spectra of MESA with SSA solutions, and the dashed lines show those of MESA without albumin. The spectra for the lowest pH (5.9) are marked with red lines and the highest pH (10.4) are marked with blue ones. The fluorescence intensity of MESA solutions with SSA increased with pH values up to pH 9 (green line). Similar to those for HSA and BSA, this increase could be attributed to the fact that λ_{ex} = 375 nm mainly excited the dissociated form of MESA. The relative increase in the fluorescence intensity of MESA with SSA as compared to MESA was about 5-fold for pH 9.5 and was similar to the increase noted for BSA in the entire pH range. At pH 5.9, the maximum value was 472 nm and this value increased with the pH up to pK_a. Above pK_a, the maximum was fixed at 483 nm. Again, as those in the case of HSA and BSA, the maximum position suggests that MESA preferred the hydrophobic sites of SSA. For the remaining excitation wavelengths, similar results were obtained. The QYs of the MESA solution with SSA are shown in Fig. 4 in green. Similar to the case of BSA, the QY decreased with increasing pH. The highest QY was noted for pH 5.9, which was 0.0089 ± 0.0002. The lowest value was observed at pH 10.4, which was

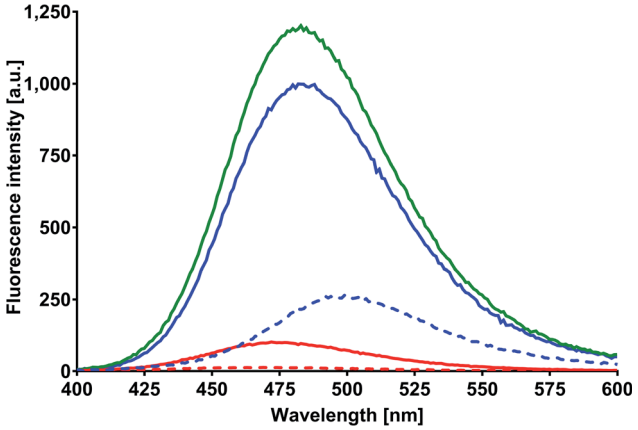

Fig. 7 Corrected fluorescence spectra of MESA with (dashed line) and without SSA (solid line). Concentration of MESA: 15 μM; concentration of SSA: 10 μM; $\lambda_{ex} = 375$ nm; 1 cm quartz cell; right-angle geometry. Red line: pH 5.9; blue line: pH 10.9.

0.0035 ± 0.0005. As compared to MESA without albumin, the QY for the lowest pH value was about 5 times higher. This ratio decreases with increasing pH up to pK_a, where it is about 3.2. Then, it rises to 5 for the highest pH. Similar to the case of the previously analyzed results, the emission spectra of MESA with SSA were subjected to Gaussian decomposition in order to obtain information on the number of complexes. Fig. S11† shows the peak positions of the individual complexes. The KS1 complex is depicted in red: its maximum value varies from 490 to 506 nm. The KS2 complex is depicted in blue, and its maximum value varies from 471 to 475 nm. The maxima of the dissociated form of MESA are marked with the light green color. The dashed line corresponds to $\lambda_{ex} = 410$ nm; the solid line, $\lambda_{ex} = 390$ nm; and the dotted line, $\lambda_{ex} = 375$ nm. Similar to that in the case of BSA, the best Gaussian fitting in the entire pH range was obtained for two complexes. This does not exclude the existence of the third complex, since its absorption band may lie below $\lambda_{ex} = 375$ nm. However, this is less likely than that in the case of BSA, because the maxima positions for this excitation are consistent with the positions observed for other excitations. The maximum of KS1 increased with the pH. At pH above 9.5, new maxima were separately formed for excitations at 390 and 410 nm. For $\lambda_{ex} = 375$ nm, the maximum was 507 ± 5 nm; for $\lambda_{ex} = 390$ nm, 496 ± 5 nm; and for $\lambda_{ex} = 410$ nm, 493 ± 2 nm. Taking this into account, it cannot be unambiguously determined whether the binding site is hydrophobic at alkaline pH. As discussed earlier, for SSA, the decay times were obtained using the global method for the three observation wavelengths and three lifetimes. The results are shown in Table 4. These lifetimes are many times greater than the MESA lifetimes; therefore, they must be associated with the complexes. The analysis of the results allowed linking τ_1 with the binding site KS1, and τ_2 and τ_3 with binding site KS2. These results support the earlier suggestions that MESA can be used as a fluorescent probe for hydrophobic albumin sites even at alkaline pH, but for excitations above 390 nm. The maximum of KS2 did not significantly change in the entire pH range under consideration

Table 4 Fluorescence decay times of MESA with SSA

pH	τ_1 [ns]	τ_2 [ns]	τ_3 [ns]
5.9	3.254	0.427	0.107
6.8	2.008	0.329	0.097
7.3	1.828	0.323	0.096
7.7	1.379	0.314	0.094
8.2	1.287	0.361	0.105
8.7	1.350	0.412	0.120
9.1	1.521	0.482	0.142
9.6	1.438	0.487	0.147
10.1	1.419	0.524	0.158
10.4	1.415	0.532	0.161

and it was about 473 nm. This suggests that the KS2 microenvironment is more hydrophobic than that of KS1.

On the other hand, the lifetimes associated with KS2 increased by about 50% in the pH range from pK_a to pH 10.4; therefore, this hypothesis cannot be confirmed without further research.

Fluorescence of MESA with RSA

MESA with RSA solutions were excited in the same manner as those done for HSA, BSA, and SSA. Fig. 8 shows the emission spectra of MESA with RSA and without RSA for $\lambda_{ex} = 375$ nm. The MESA spectra with RSA are marked with solid lines and the MESA spectra without albumin are marked with dashed lines. The spectra plotted for the lowest pH (5.9) are depicted in red, and those plotted for the highest pH (10.4) are in blue, whereas the spectrum for the highest intensity is denoted in green. The fluorescence intensity increased as the pH increased to 9 (Fig. 8, green line), after which it started to decrease. This effect is probably related to the increased concentration of the dissociated form of MESA, and it was also observed in solutions with the other proteins. An increase was observed in the fluorescence intensity as compared to the MESA solution without proteins, which was equal to 6.8 at pH 9.6; this was distinctly greater than

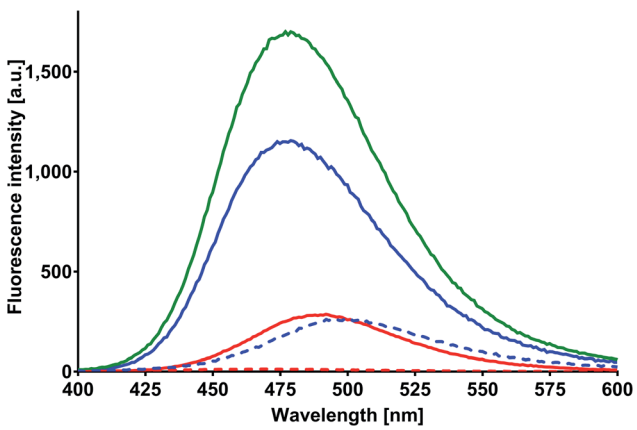

Fig. 8 Corrected fluorescence spectra of MESA with (dashed line) and without (solid line) RSA. Concentration of MESA: 15 μM; concentration of RSA: 10 μM; $\lambda_{ex} = 375$ nm; 1 cm quartz cell; right-angle geometry. Red line: pH 5.9; blue line: pH 10.9.

Table 5 Fluorescence decay times of MESA with RSA

pH	τ_1 [ns]	τ_2 [ns]	τ_3 [ns]
5.9	3.399	0.719	0.214
6.8	2.751	0.683	0.195
7.3	2.274	0.655	0.183
7.7	1.793	0.612	0.169
8.2	1.465	0.566	0.159
8.7	1.399	0.563	0.162
9.0	1.346	0.556	0.165
9.6	1.421	0.612	0.182
10.1	1.474	0.654	0.199
10.4	1.415	0.615	0.191
10.9	1.919	0.731	0.218

the increase noted for BSA and SSA and significantly lower than that noted for HSA. Unlike other proteins, the fluorescence maximum of MESA with RSA moved toward the shorter wavelengths as the pH increased to pK_a: for pH 5.9, it was 492 nm; above pK_a, it oscillated at around 478 nm. These results suggest that in RSA, MESA also preferred the hydrophobic binding sites.

The QY of the MESA solution with RSA is shown in Fig. 4 (denoted in violet color). Similar to those for SSA and BSA, the QY of MESA with RSA decreased with increasing pH. For the lowest pH (5.9), it was 0.0261 ± 0.0008; for the highest pH (10.4), it was 0.00035 ± 0.00005. The greatest increase in QY, in relation to MESA solutions without albumin, was 16 times and it was achieved at pH 5.9. Along with the increase in pH to the pK_a value, the ratio dropped to 4.8 at pH 8.7. Above pK_a, it increased to 5.6 at pH 10.4. These results confirm that MESA can also be used as an RSA fluorescent probe in the pH range from 5.9 to 10.4.

Similar to the spectra of MESA with the other proteins, the fluorescent spectra with RSA were decomposed into Gaussian peaks. The results are shown in Fig. S12.† The KR1 complex is denoted in red, which has its maxima ranging from 487 to 500 nm. The KR2 complex is denoted in blue and its maximum is between 491 and 466 nm. The position of the fluorescence maxima of the dissociated form of MESA is denoted in light green. The solid lines indicate the maxima for λ_{ex} = 390 nm; dashed lines, 410 nm; and dotted ones, 375 nm. The best matches were obtained for the two-band distribution. If there was a third complex, its emission band should have been observed for excitations below 375 nm. The location of the maximum KR1 remained approximately constant with respect to the pK_a value and ranged from 492 to 497 nm; above pK_a, it oscillated for various excitations. The induction of relatively large errors caused its location to be indeterminable. The maximum of KR2 did not change till reaching pK_a and it was 488 nm. Above pK_a, this value shifted toward shorter wavelengths and reached 468 nm at pH 10.4. These results suggest that both the binding sites are not unambiguously hydrophobic.

Fluorescence decay times were also measured for RSA and the results were obtained using the procedure as that used above for λ_{ex} = 375 nm. The best matches were obtained for the triple-exponential decay. The results are listed in Table 5. The analysis of lifetimes dependence on the pH values shows that above pK_a, all the three lifetimes showed similar changes. This suggests that the MESA microenvironments at the KR1 and KR2 binding sites were similar.

Binding study

In order to obtain the binding constants between the serum albumins and MESA, steady-state fluorescence spectra and time-resolved fluorescence decays of serum albumins were measured at pH 7.4 and λ_{ex} = 280 nm. The corrected emission spectra of HSA in the presence of MESA (Fig. S13†) show a significant decrease in intensity, which indicated the presence of either dynamic or static quenching. The number of calculated lifetimes was not dependent on the number of Trps in albumin. In HSA, BSA, and SSA, this value was 2; in RSA, it was 3. Table 6 lists the τ_0 values computed for the different albumins. The τ and τ_0 values were amplitude-weighted lifetimes.[24] Their values slightly differed, which suggests that for BSA and SSA, as compared to HSA, two Trps have similar lifetimes; this, in turn, suggests that the microenvironment was similar for both of them. Three lifetimes for RSA suggested the fluorescence of tyrosine (Tyr). Fig. 9 shows the Stern–Volmer plots for HSA: both $\frac{F_0}{F}$ and $\frac{\tau_0}{\tau}$. Since the X axis and $\frac{\tau_0}{\tau}$ are parallel to each other, the observed quenching is static rather than dynamic. Similar plots were obtained for the other albumins. Quenching constants K_{SV} and k_q were determined from eqn (2) ($R^2 > 0.99$), as listed in Table 6. Values of k_q for each albumin were significantly higher than the reported maximal diffusive quenching constant k_q (1.2×10^{10} M^{-1}).[24] This suggests that a complex existed in the ground state, which was confirmed by the absorption spectra (Fig. 1 and S2†).

Fig. 10 shows the dependence of $\log[Q]$ on $\log\left[\frac{F_0 - F}{F}\right]$ for determining the quenched fluorescence of HSA. The binding constant, K_b, and the number of binding sites, n, determined from eqn (3) ($R^2 > 0.99$) are listed in Table 6. All the obtained K_b values were higher than those for Sa and BSA (K_b = 600 M^{-1}).[28] The K_b value for HSA was about 28 times higher than those for

Table 6 Results of Stern–Volmer and FRET analyses for the different proteins

Protein	τ_0 [ns]	K_{SV} [M^{-1}]	$k_q \times 10^{-11}$ [s^{-1} M^{-1}]	K_b [M^{-1}]	n	R_0 [Å]	r [Å]
HSA	6.35 ± 0.14	66 700 ± 2200	105.0 ± 4.2	$52\,000^{+2200}_{-1500}$	0.97 ± 0.03	23.0	24.7
BSA	5.90 ± 0.10	9290 ± 180	15.75 ± 0.41	1800^{+1100}_{-700}	0.84 ± 0.04	21.2	33.9
SSA	5.48 ± 0.16	29 280 ± 660	53.4 ± 2.0	$10\,500^{+5400}_{-3600}$	0.90 ± 0.04	22.7	30.4
RSA	3.35 ± 0.17	5560 ± 240	16.60 ± 1.1	1800^{+1600}_{-800}	0.89 ± 0.06	19.5	36.7

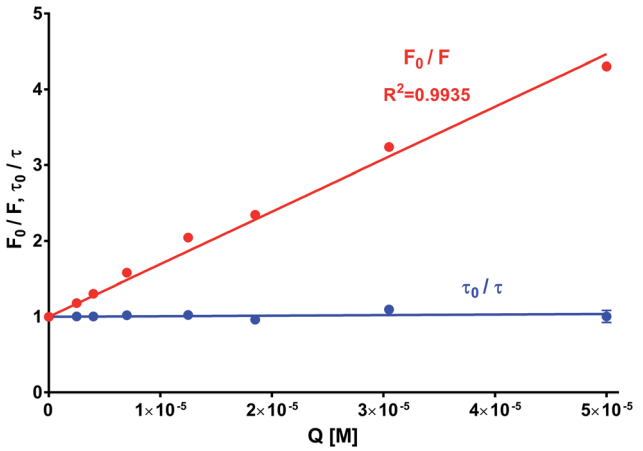

Fig. 9 Stern–Volmer plot of HSA with MESA. Concentration of HAS: 5 μM; concentration of MESA: 2.5–50.0 μM; λ_{ex} = 280 nm; λ_{em} = 350 nm; 1 cm quartz cell; right-angle geometry.

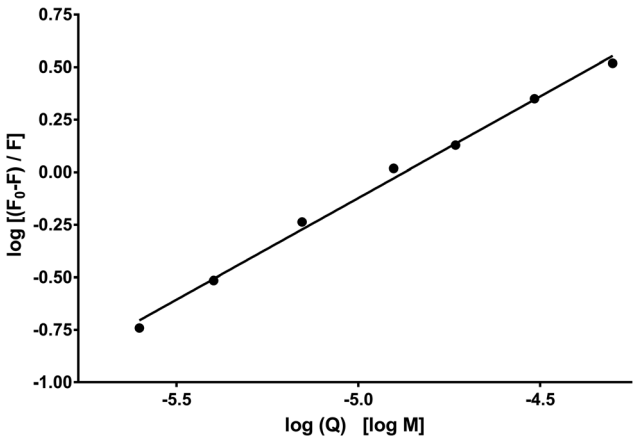

Fig. 10 Dependence of log[(F_0 − F)/F] on log[Q] for HSA with MESA. F_0 and F: fluorescence of donor (HSA) without and with MESA, respectively. Concentration of HAS: 5 μM; concentration of MESA: 2.5–50.0 μM; λ_{ex} = 280 nm; λ_{em} = 350 nm; 1 cm quartz cell; right-angle geometry.

BSA and RSA and about 5 times higher for SSA. This is in agreement with the fluorescence results obtained from the spectral analysis. The number of binding sites (n) for all the albumins was below one (Table 6), confirming that there was only one binding site. These results are inconsistent with the results from the spectral decomposition and time-resolved spectroscopy data, which suggested a higher number of binding sites. In order to get an additional insight into the location of the binding pockets in the proteins, the FRET theory was employed to determine the distance between MESA and Trp in the albumins. The Förster distance, R_0, was determined using eqn (4) and listed in Table 6. Then, it was used to calculate the distance (r) between Trp in serum albumins and bound MESA (Table 6). For each albumin, r was smaller than 8 nm; for HSA, BSA, and SSA, $r < 1.5R_0$, which proves that resonance energy transfer was possible and could be significant. The r values calculated for HSA reveals that the most probable binding site is Sudlow site I, which is close to the Trp in HSA.[25,26] In the case of BSA (with two Trps), it is unclear which binding site is preferred by MESA; however, reports have indicated a similar r value for molecules preferring Sudlow site I.[27]

Summary

Results obtained for all the tested albumins showed many similarities. MESA formed complexes with all the albumins in the pH range from 5.9 to 11. Complex formation with albumins did not significantly affect pK_a, suggesting a small contribution of the MESA hydroxyl group. The complexes had their own absorption and fluorescence bands. The maxima of the fluorescence bands were blue-shifted as compared to those of the unbound MESA, which suggests their hydrophobic nature. In the case of HSA, BSA, and SSA, the fluorescence maxima were red-shifted as the pH increased up to pK_a. Above the pK_a value, the maxima remained unchanged. The highest intensities were observed in the pH range from 9.0 to 9.5. Also, QY determined for complexes with BSA, SSA, and RSA showed similar increases as compared to the unbound MESA. Large differences were observed in the fluorescence intensity, QYs, and K_b values of the complexes with HSA as compared to those with the other proteins. In turn, the blue-shift of the fluorescence band with the increase in pH up to pK_a was observed only for RSA. Some analyses showed that there was a different number of binding sites in different proteins, *i.e.*, three for HSA, two (with a potential third) for BSA, and two for both SSA and RSA. However, the analysis conducted using eqn (3) indicated the existence of only one binding site in all the albumins.

It is interesting whether four protein binding sites can be treated as similar or the same, *i.e.*, whether KH1, KB1, KS1, and KR1 complexes could be considered as K1 binding sites. Similarly, whether KH2, KB2, KS2, and KR2 could be considered as K2 binding sites. Unfortunately, the answer is ambiguous. First, complexes with RSA must be excluded from this juxtaposition, which, despite certain similarities, behave differently: although the blue-shift in the KR2 complex maximum occurred with an increase in pH, all the lifetime values changed in the same way

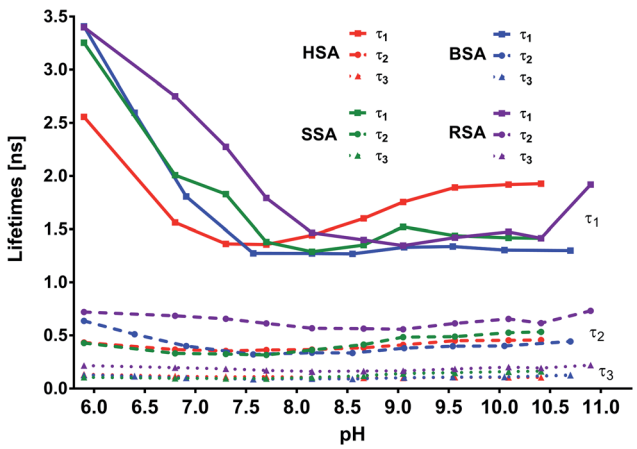

Fig. 11 Calculated lifetimes for MESA with and without albumins *versus* pH.

above pK_a. Differences were also found between the binding sites of the other three proteins. Below pK_a, there was a greater blue-shift in the KH2 maxima as compared to MESA than those in KB2 and KS2. The maxima of the complexes vary with changes in the pH value. In BSA and SSA, the KB1 and KS1 maxima would reduce their blue-shifts with increasing pH, while the maxima positions of KB2 and KS2 did not change. An opposite behavior was observed in HSA, namely, the KH2 blue-shift decreased with increasing pH, while the positions of the KH1 maxima did not change.

In addition to the abovementioned differences, similarities could also be noticed, particularly for lifetime matches (Fig. 11). First, for complexes with all the tested albumins, the best fit for the decay times was obtained using the triple exponential. Second, for MESA with HSA, BSA, and SSA, the τ_1 values ranged from 1.2 to 3.5 ns; τ_2, from 0.3 to 0.65 ns; and τ_3, from 0.085 to 0.17 ns. However, the differences for individual pH values were significantly smaller (Tables 2–4). Third, there were similarities in the course of the individual values of τ_1, τ_2, and τ_3 at pH values for the different proteins, particularly those above pK_a.

Fourth, for complexes with HSA, BSA, and SSA, it could be noticed that τ_1 was linked to the KH1, KB1, and KS1 complexes. Analogously, the binding sites of KH2, KB2, and KS2 could be connected to τ_2 and τ_3. Fifth, the results for both BSA and HSA reveal that MESA prefers Sudlow site I. When analyzing the decomposition of the fluorescence spectra into Gaussian peaks, the similarity of the maxima of the fluorescence bands of the complex associated with the K2 binding sites above pK_a can be noticed—they remained constant and ranged from 465 to 475 nm for λ_{ex} = 390 nm. For complexes related to the K1 binding site, fitting errors prevented a similar analysis.

In summary, it seems reasonable to accept the hypothesis that we are referring to binding sites of the same nature—with similar microenvironments—particularly those above pK_a. However, further studies are required to confirm this hypothesis.

Increasing the pH above 7 causes a less rigid structure of albumins,[31] *e.g.*, BSA has a very high α-helix content (~62%) in the N-form, which decreases to ~44% in the B-form and 2% in the A-form. In the A-form, the structure of BSA developed in the random coil conformation. The obtained data indicate that protein unfolding up to pH 10 did not cause the unbonding of the MESA. Above pH 10, the complex gradually disappeared, which can be caused by the disappearance of the hydrophobic pockets and a high negative net charge on the protein. Such a behavior up to pH 10 indicated the strong affinity of MESA toward the albumins. In contrast, completely dissociated hydroxy and carboxy groups at alkaline pH in the Sa molecule resulted in the fact that no complex was formed with BSA.[28]

Conclusions

The results obtained from the absorption and fluorescence analyses confirmed the formation of MESA molecular complexes with the studied albumins in the examined pH range from 5.9 to 10.7. Changes in the absorption spectra and pK_a values revealed the formation of complexes in the electronic ground state, which resulted in a significant increase in the fluorescence intensity and QY for MESA in the presence of proteins, particularly with HSA. The blue-shift in the fluorescence spectra as compared to unbound MESA suggests that MESA prefers the hydrophobic binding sites. Together with the increase in the fluorescence decay times, this indicated the feasibility of using MESA as a fluorescent probe of hydrophobic binding sites of albumins, particularly at alkaline pH.

The Gaussian decomposition of the fluorescence spectra and lifetimes suggests the existence of at least two types of binding sites in all the albumins, in contrast to the single site obtained from the fluorescence quenching experiments. At higher pH, the dissociation of hydrogen from the hydroxyl group of MESA and the high negative net charge on the proteins did not hinder the formation of complexes. Binding constants were calculated for MESA with HSA, BSA, SSA, and RSA, which were 52 000, 1800, 1050, and 1800 M^{-1}, respectively, and were significantly higher than that in the case of the binding constants computed for Sa and BSA.[28] This indicated that blocking the protein dissociation from the carboxyl group increased the binding affinity.

Conflicts of interest

There are no conflicts to declare.

Acknowledgements

Project financially supported by Minister of Science and Higher Education in the range of the program entitled "Regional Initiative of Excellence" for the years 2019–2022, Project No. 010/RID/2018/19, amount of funding 12 000 000 PLN. We would also like to acknowledge the support from the project No. 17.610.011-110.

Notes and references

1 Y. Takaya, Y. Kondo, T. Furukawa and M. Niwa, *J. Agric. Food Chem.*, 2004, **51**, 8061–8066.
2 Y. Chen, H. Xiao, J. Zheng and G. Liang, *PLoS One*, 2015, **10**(3), e0121276.
3 M. Foti, C. Daquino and C. Geraci, *J. Org. Chem.*, 2004, **69**, 2309–2314.
4 O. Koroleva, A. Torkova, I. Nikolaev, E. Khrameeva, T. Fedorova, M. Tsentalovich and R. Amarowicz, *Int. J. Mol. Sci.*, 2014, **15**, 16351–16380.
5 J. Teixeira, A. Gaspar, E. M. Garrido, J. Garrido and F. Borges, *BioMed Res. Int.*, 2013, **2013**, 251754.
6 C. Manach, A. Scalbert, C. Morand, C. Rémésy and L. Jimenez, *Am. J. Clin. Nutr.*, 2004, **79**, 727–747.
7 N. Niciforovic and H. Abramovic, *Compr. Rev. Food Sci. Food Saf.*, 2013, **13**, 34–51.
8 A. Siger, J. Czubinski, K. Dwiecki, P. Kachlicki and M. Nogala-Kalucka, *Eur. J. Lipid Sci. Technol.*, 2013, **115**, 1130–1138.

9 S. M. Kern, R. N. Bennett, P. W. Needs, F. A. Mellon, P. A. Kroon and M.-T. Garcia-Conesa, *J. Agric. Food Chem.*, 2003, **51**, 7884–7891.
10 B. A. Acosta-Estrada, J. A. Gutiérrez-Uribe and S. O. Serna-Saldívar, *Food Chem.*, 2014, **152**, 46–55.
11 L. Trnkova, I. Bousova, V. Kubicek and J. Drsata, *Nat. Sci.*, 2010, **2**, 563–570.
12 S.-K. Chung, T. Osawa and S. Kawakishi, *Biosci., Biotechnol., Biochem.*, 1997, **61**, 118–123.
13 A. Gaspar, M. Martins, P. Silva, E. M. Garrid, J. Garrido, O. Firuzi, R. Miri, L. Saso and F. Borges, *J. Agric. Food Chem.*, 2010, **58**, 11273–11280.
14 S. M. Kern, R. N. Bennett, F. A. Mellon, P. A. Kroon and M.-T. Garcia-Conesa, *J. Agric. Food Chem.*, 2003, **51**, 6050–6055.
15 C. Chen, *Oxid. Med. Cell. Longevity*, 2016, **2016**, 3571614.
16 X.-L. Jin, X. Wei, F.-M. Qi, S.-S. Yu, B. Zhou and S. Bai, *Org. Biomol. Chem.*, 2012, **10**, 3424–3431.
17 J. Fan, X. Chen, Y. Wang, C. Fan and Z. Shang, *J. Zhejiang Univ., Sci., B*, 2006, **7**, 452–458.
18 A. Papadopoulou, R. J. Green and R. A. Frazier, *J. Agric. Food Chem.*, 2005, **53**, 158–163.
19 Y. Zhang, S. Wu, Y. Qin, J. Liu, J. Liu, Q. Wang, F. Ren and H. Zhang, *Food Chem.*, 2018, **240**, 1072–1080.
20 D. C. Carter and J. X. Ho, *Adv. Protein Chem.*, 1994, **45**, 153–203.
21 B. Smyk, G. Mędza, A. Kasparek, M. Pyrka, I. Gryczynski and M. Maciejczyk, *J. Phys. Chem. B*, 2017, **121**, 7299–7310.
22 M. Fujita, M. Yamada, S. Nakajima, K. Kawai and M. Nagai, *Chem. Pharm. Bull.*, 1984, **32**, 2622–2627.
23 A. Kasparek and B. Smyk, *Spectrochim. Acta, Part A*, 2018, **198**, 297–303.
24 J. R. Lakowicz, *Principles of Fluorescence Spectroscopy*, Springer, Singapore, 3rd edn, 2009.
25 S. Ranjbar, Y. Shokoohinia, S. Ghobadi, N. Bijari, S. Gholamzadeh, N. Moradi, M. R. Ashrafi-Kooshk, A. Aghaei and R. Khodarahmi, *Sci. World J.*, 2013, **2013**, 305081.
26 R. Joshi, M. Jadhao, H. Kumar and S. K. Ghosh, *Bioorg. Chem.*, 2017, **75**, 332–346.
27 H.-x. Zhang, Y. Zhou and E. Liu, *Spectrochim. Acta, Part A*, 2012, **92**, 283–288.
28 B. Smyk, *J. Fluoresc.*, 2003, **13**, 349–356.
29 Z. Wieczorek, J. Stepinski, M. Jankowska and H. Lönneberg, *J. Photochem. Photobiol., B*, 1995, **28**, 57–63.
30 N. Fogh-Andersen, P. J. Bjerrum and O. Siggaard-Andersen, *Clin. Chem.*, 1993, **39**, 48–52.
31 N. Varga, V. Hornok, D. Sebök and I. Dékány, *Int. J. Biol. Macromol.*, 2016, **88**, 51–58.

